In Situ Mass Spectrometric Detection of Interfacial Intermediates in the Oxidation of RCOOH(aq) by Gas-Phase OH-Radicals

ARTICLE *in* THE JOURNAL OF PHYSICAL CHEMISTRY A · MAY 2014

Impact Factor: 2.69 · DOI: 10.1021/jp503387e · Source: PubMed

3 AUTHORS, INCLUDING:

Michael R. Hoffmann
California Institute of Technology
390 PUBLICATIONS **30,232** CITATIONS

SEE PROFILE

Agustin J Colussi
California Institute of Technology
222 PUBLICATIONS **4,230** CITATIONS

SEE PROFILE

THE JOURNAL OF PHYSICAL CHEMISTRY A

Article

pubs.acs.org/JPCA

In Situ Mass Spectrometric Detection of Interfacial Intermediates in the Oxidation of RCOOH(aq) by Gas-Phase OH-Radicals

Shinichi Enami,*[,†,‡,§] Michael R. Hoffmann,[‖] and Agustín J. Colussi[‖]

[†]The Hakubi Center for Advanced Research, Kyoto University, Kyoto 606-8302, Japan

[‡]Research Institute for Sustainable Humanosphere, Kyoto University, Uji 611-0011, Japan

[§]PRESTO, Japan Science and Technology Agency, Kawaguchi 332-0012, Japan

[‖]Linde Center for Global Environmental Science, California Institute of Technology, Pasadena, California 91125, United States

Supporting Information

ABSTRACT: Products and intermediates of the oxidation of aqueous alkanoic acids initiated by gas-phase hydroxyl radicals, ·OH(g), at the air−water interface were detected by mass spectrometry in a novel setup under various experimental conditions. Exposure of submillimolar RCOOH (R = methyl, *n*-pentyl, *n*-heptyl) aqueous microjets to ∼10 ns ·OH(g) pulses from the 266 nm laser flash photolysis of $O_3(g)/O_2(g)/H_2O(g)$ mixtures yielded an array of interfacial species that were unambiguously and simultaneously identified in situ by online electrospray mass spectrometry. We found that peroxyl radicals $R(-H)(COO^-)OO\cdot$ react within 50 μs to produce alcohols $R(-H)(COO^-)OH$ and carbonyls $R(-2H)(COO^-)=O$ via competitive Russell and Bennett−Summers mechanisms. We confirmed the formation of hydroperoxides $R(-H)(COO^-)OOH$ in experiments performed in D_2O. To our knowledge, this is the first report on the prompt and simultaneous detection of products and peroxyl/peroxide intermediates in the heterogeneous oxidation of aqueous organics initiated by ·OH(g).

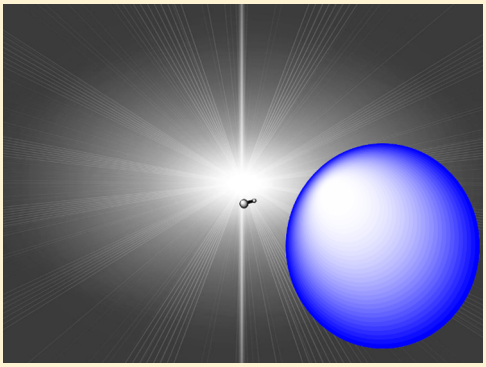

INTRODUCTION

Environmental organic surfaces exposed to ambient air inevitably undergo oxidative degradation.[1] Prominent among such surfaces, on account of their large surface-to-volume ratios, are those of tropospheric organic aerosol particles.[2] Such particles typically consist of internally or externally mixed hydrophobic and amphiphilic substances within an aqueous matrix. Whereas unsaturated moieties are susceptible to direct attack by major gas-phase oxidants, such as ozone and nitrogen dioxide, the degradation of alkyl groups is initiated by more reactive trace species such as the short-lived gas-phase hydroxyl radicals, ·OH(g). As the keystone of atmospheric chemistry,[3] the reactions of ·OH(g) with gas-phase organic species, and the processes triggered by such interactions have been investigated extensively.[4,5] It has become increasingly apparent, however, that heterogeneous processes play unique and essential roles in the troposphere.[6−9] For example, the progressive oxidation of saturated organics on the surfaces of aerosol particles in humid atmospheres increases their hygroscopicities and hydrophilicities,[10−13] and, hence, their ability to nucleate water vapor. As a result, the oxidative aging of condensed-phase organics by ·OH(g) has received much attention recently.[14−25] However, most, if not all, such studies consisted of exposing organic solids in the form of particles or films to ·OH(g) for prolonged periods, followed by product detection. The mechanisms proposed to account for the products detected in such gas−solid events were generally assumed to be similar to those developed for the putatively similar processes in fluid solutions, which proceed via the intermediacy of alkyl peroxyl radicals.

Previously, we have utilized the high sensitivity, surface selectivity and unambiguous identification capabilities of online electrospray mass spectrometry (ES-MS)[26−29] to characterize in situ the intermediates and products formed on the surfaces of continuously flowing, uncontaminated liquid microjets exposed to gas-phase reactive gases (i.e., $O_3(g)$) beams for ∼10−50 μs under ambient conditions (i.e., at 1 atm total pressure, 298 K).[26,28,30−33] Herein, we extend the scope of our experiments to include short-lived, gas-phase radical reactants, which we generate via laser flash photolysis of appropriate precursor mixtures in the immediate vicinity of the liquid microjets.

EXPERIMENTAL SECTION

Methods. Figure 1 shows a schematic diagram of the experimental setup.

The prompt (within the ∼10−50 μs lifetime of the intact microjets; see below) formation of anionic products from the reaction of aqueous reactants with gaseous species at 1 atm at

Received: April 7, 2014
Revised: May 11, 2014
Published: May 19, 2014

   dx.doi.org/10.1021/jp503387e | J. Phys. Chem. A 2014, 118, 4130−4137

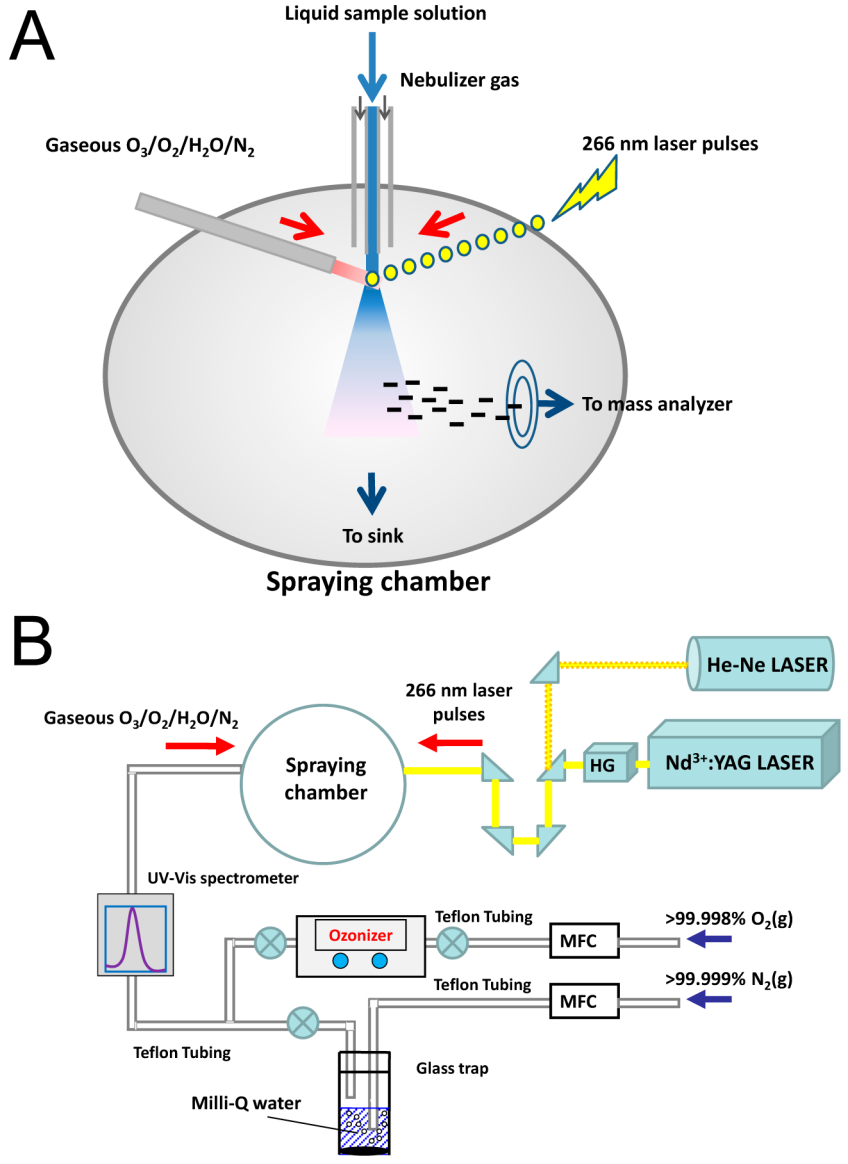

Figure 1. Schematic diagram of our setup. It allows for the in situ monitoring of reactions of laser-generated gas-phase radical species on the surface of aqueous solutions. HG stands for harmonic generator; MFC, for mass flow controller.

298 K are monitored in situ by an electrospray mass spectrometry (ES-MS, Agilent 6130 Quadrupole LC/MS Electrospray System, Kyoto University). Aqueous solutions are pumped (100 μL min^{-1}) into the spraying chamber of the mass spectrometer through a grounded stainless steel needle (100 μm bore) coaxial with a sheath issuing nebulizer N_2(g) at high gas velocity ($v_g \sim 160$ m/s).[26] The surface specificity of our experiments had been previously demonstrated by showing that (i) anion signal intensities I in the mass spectra of *equimolar* salt solutions adhere to a normal Hofmeister series rather than being identical, e.g., $I(ClO_4^-) > I(I^-) > I(Br^-)$,[27,34−37] (ii) the depth of the sampled interfacial layers can be controlled by varying the nebulizer gas velocity v_g, as evidenced by the fact that ion signal intensities *and* relative anion surface affinities increase with higher gas velocities v_g and extrapolate to zero as $v_g \rightarrow 0$,[26] and (iii) they allow the detection of products of gas−liquid reactions that could only be formed at the air−water interface.[28,30,31,33,38] Note that the products we observe are formed when gaseous reactants collide with the intact aqueous jets as they emerge from the nozzle, i.e., before jets are broken up into submicrometer droplets by the nebulizer gas (see the Supporting Information for further details).[33]

Ozone is produced from ultrapure O_2(g) (purity >99.998%) flowing at 1.0 standard liters per minute through a high-pressure discharge ozonizer (KSQ-050, Kotohira). The O_3(g) concentration is quantified online by a UV−vis absorption spectrophotometry at 250 and 300 nm, (absorption cross sections $\sigma = 1.1 \times 10^{-17}$ and 3.9×10^{-19} cm^2 $molecule^{-1}$, respectively)[39] prior to entering the reaction chamber (Figure 1). Throughout, the reported [O_3(g)] values correspond to the concentrations actually sensed by the microjets in the reaction chamber, which are ~11 times smaller than those determined upstream UV absorbances due to dilution by the drying gas. H_2O(g) is carried into the chamber via a known flow of N_2(g) saturated by sparging milli-Q water (Figure 1). We assume that the chamber was saturated with H_2O(g) at 298 K throughout.

The 266 nm beam emitted by our Nd^{3+}:YAG laser setup (LOTIS TII, LS-2131M-10 with a harmonic generator assembly HG-TF, pulse duration 8 ± 1 ns, 266 nm beam

dx.doi.org/10.1021/jp503387e | J. Phys. Chem. A 2014, 118, 4130−4137

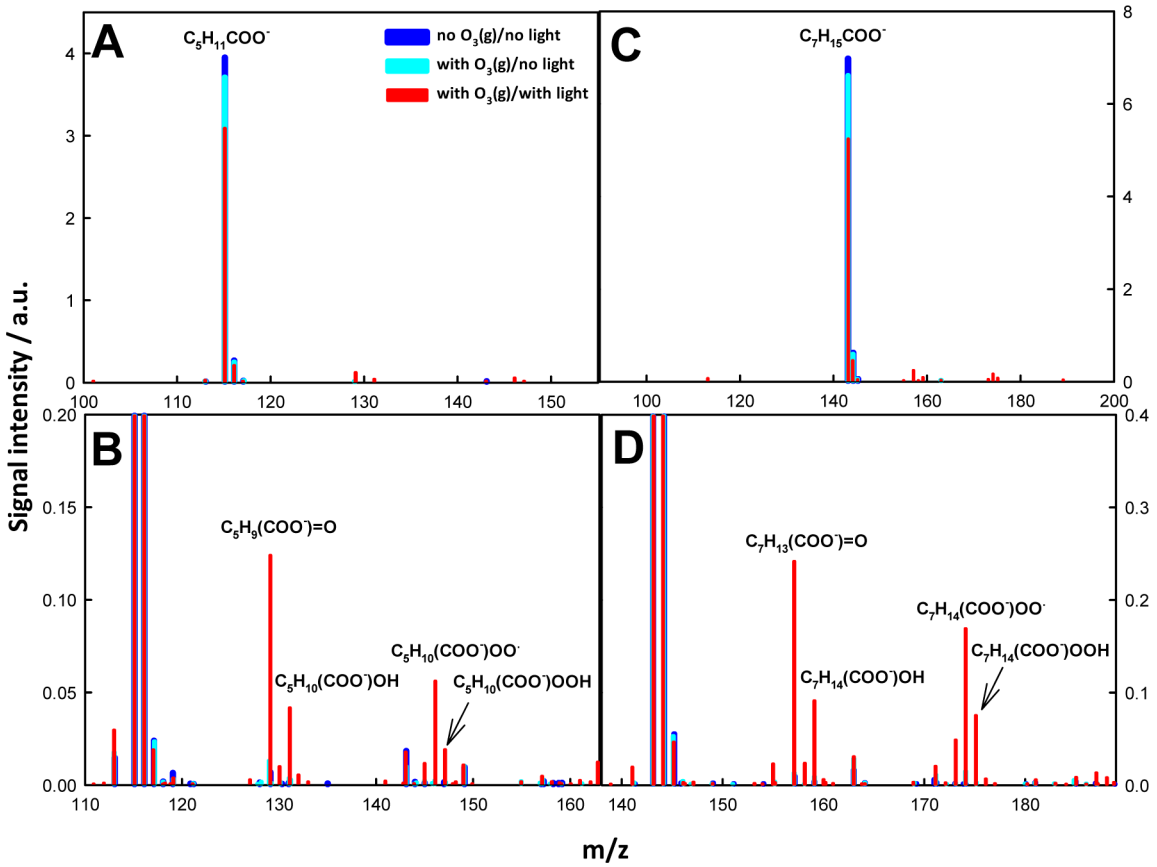

Figure 2. Negative ion electrospray mass spectra of 0.1 mM (pH 4.8) hexanoic acid (A, B) or octanoic acid (C, D) microjets exposed to 650 ppmv $O_3(g)$ in $O_2(g)/H_2O(g)/N_2(g)$ mixtures at 1 atm and 298 K. Cyan: laser off. Red: under 40 mJ, ~8 ns pulses (at 10 Hz) of 266 nm radiation. 1 ppmv = 2.46×10^{13} molecules cm^{-3}.

diameter 10.0 ± 1.0 mm, beam divergence ≤1.5 mrad, 10 Hz) is used to generate ·OH(g) at or near the gas−liquid interface (Figure 1). The 266 nm laser beam energies are measured with a power meter (OPHIR, NOVA II, sensor:3A-P-V1-ROHS). The 266 nm beam energy can be tuned up to 40 mJ $pulse^{-1}$. The laser beam is introduced into the spraying chamber via quartz prisms (synthetic fused silica, refractive index n_d = 1.458) on kinematic prism holders (SIGMAKOKI Co., Ltd., Japan) and finely aligned with a He−Ne laser (Melles Griot, 05-LHP-111, 632.8 nm CW) beam, which becomes visible as it is scattered upon hitting the liquid jet.

Experimental conditions were as follows: drying gas flow rate, 13 L min^{-1}; drying gas temperature, 340 °C; inlet voltage, + 3.5 kV relative to ground; fragmentor voltage value, 80 V. CH_3COOH (purity >99.7%), $C_5H_{11}COOH$ (>99%), and $C_7H_{15}COOH$ (>98%) were purchased from Nacalai Tesque (Kyoto, Japan). D_2O (99.9%) and $H_2{}^{18}O$ (97%) were purchased from Sigma-Aldrich and Santa Cruz Isotope, respectively. All solutions were prepared in purified water (Resistivity ≥18.2 MΩ cm at 298 K) from a Millipore Milli-Q water purification system. The pH of solution was measured by a calibrated pH meter, Horiba LAQUA F-74, before the experiments. All experiments were performed at 298 ± 2 K.

Estimation of ·OH Radical Concentration. The dissociation of $O_3(g)$ by 266 nm photons into $O(^1D)$, followed by the reaction of $O(^1D)$ with $H_2O(g)$, in competition with its deactivation by $N_2(g)$ and $O_2(g)$ into $O(^3P)$, promptly yields ·OH(g).[40] We estimate that under our experimental conditions 0.1−10% $O_3(g)$ is converted in ·OH(g) (see below). The concentration of ·OH hitting the microjet is derived from the $O_3(g)$ absorption cross sections, laser fluence, and reported gas-phase kinetic parameters. Because the number of photons is always larger than the number of $O_3(g)$ molecules under present conditions, we estimate the initial $O(^1D)$ concentrations from 266 nm photolysis from Beer's law:

$$\ln(N_0/N) = I_0\sigma\Phi_{dis} \quad \text{(E1)}$$

$$N = N_0 \exp(-I_0\sigma\Phi_{dis}) \quad \text{(E2)}$$

where σ is the absorption cross section, Φ_{dis} is the dissociation quantum yield, I_0 is the laser fluence in number of photons per unit area, N_0 is the number of molecules before laser irradiation, and N is the number of molecules after laser irradiation.[41] We derive $N/N_0 \sim 0.5$, meaning $[O(^1D)]_0 \approx 0.5[O_3(g)]$ at the highest 266 nm laser pulse energy ~40 mJ $pulse^{-1}$. $O(^1D)$ reacts with excess $H_2O(g)$ ($[H_2O(g)] \sim 7.6 \times 10^{17}$ molecules cm^{-3}) to form ·OH radical within ~6 ns (from $k_1 = 2.2 \times 10^{-10}$ cm^3 $molecule^{-1}$ s^{-1}), reaction R1,[39,42]

$$O(^1D) + H_2O \rightarrow 2\cdot OH \quad \text{(R1)}$$

or is competitively deactivated by N_2 and O_2, reactions R2a and R2b

$$O(^1D) + N_2 \rightarrow O(^3P) + N_2 \quad \text{(R2a)}$$

$$O(^1D) + O_2 \rightarrow O(^3P) + O_2 \quad \text{(R2b)}$$

where $k_{2a} = 2.6 \times 10^{-11}$ and $k_{2b} = 4.0 \times 10^{-11}$ cm^3 $molecule^{-1}$ s^{-1}, respectively.[39,42] We estimate that ~20% $O(^1D)$ is

dx.doi.org/10.1021/jp503387e | J. Phys. Chem. A 2014, 118, 4130−4137

converted into ·OH radicals under present conditions. In this manner, $[\cdot OH]_0$ can be varied from a few tens of ppbv to 100 ppmv. Note that the reaction of $O(^1D)$ with RCOOH(aq) is negligible. By assuming a rate constant for such process as large as $k = 6 \times 10^{-10}$ cm^3 molecule^{-1} s^{-1},[43] we estimate that this $O(^1D)$ reaction channel at [RCOOH(aq)] = 0.1 mM = 6.02×10^{16} molecules cm^{-3}, is >20 times slower than the gas-phase reactions R1, R2a, and R2b. $O(^3P)$ is largely consumed by O_2 to regenerate O_3 ($\tau \sim 36$ μs) under present conditions.

RESULTS AND DISCUSSION

Figure 2 shows typical negative ion electrospray mass spectra of 0.1 mM aqueous *n*-hexanoic acid (HA) or *n*-octanoic acid (OA) microjets exposed to $O_3(g)/O_2(g)/H_2O(g)/N_2(g)$ mixtures with the 266 nm laser on and off.

Note that at the same 0.1 mM concentration, octanoate (n-$C_7H_{15}COO^-$, R_7COO^-) m/z = 143 signals are 1.8 times larger than the m/z = 115 hexanoate (n-$C_5H_{11}COO^-$, R_5COO^-) signals (cf. Figure 2A,C), as expected from the direct dependence of anion affinities for the air−water interface on anion size.[35,44,45] This observation supports the tenet that our experiments effectively sample interfacial layers rather than the bulk liquid, in accordance with previous results.[26,27,32,34,46,47] Exposure to >600 ppmv $O_3(g)$ in $O_2(g)/H_2O(g)/N_2(g)$ does not generate new signals, thereby confirming the inertness of these anions toward O_3.[48,49] Then, upon irradiation with 266 nm pulses we observe, as expected, the partial depletion of reactant anions and the formation of new species, which we ascribe to reactions involving ·OH. We estimate $[\cdot OH]_0 \sim 62$ ppmv in the experiments of Figure 2A−D. The molecular identity and progeny of the products can be readily inferred from their mass-to-charge ratios. In Figure 2B, the m/z = 146 = 115 − 1 + 32 signal is assigned to peroxyl radicals $R_5(-H)(COO^-)OO\cdot$, m/z = 129 = 146 − 16 − 1 to $R_5(-2H)(COO^-)$=O carbonyls, and m/z = 131 = 146 − 16 + 1 to $R_5(-H)(COO^-)OH$ alcohols. Similarly, m/z = 174 = 143 − 1 + 32 corresponds to $R_7(-H)(COO^-)OO\cdot$, m/z = 157 = 174 − 16 − 1 to $R_7(-2H)(COO^-)$=O, and m/z = 159 = 174 − 16 + 1 to $R_7(-H)(COO^-)OH$. We emphasize that the same products were observed on aqueous RCOOH microjets in the 0.01−1.0 mM range (Figure S1, Supporting Information). These results are consistent with the following mechanism, reactions R3−R9:

$$RCOO^- + \cdot OH \rightarrow \cdot R(-H)COO^- + H_2O \quad (R3)$$

$$\cdot R(-H)COO^- + O_2 + M \rightarrow R(-H)(COO^-)OO\cdot + M \quad (R4)$$

$$2R(-H)(COO^-)OO\cdot \rightarrow R(-2H)(COO^-)=O + R(-H)(COO^-)OH + O_2 \quad (R5)$$

$$2R(-H)(COO^-)OO\cdot \rightarrow 2R(-2H)(COO^-)=O + H_2O_2 \quad (R6)$$

$$2R(-H)(COO^-)OO\cdot \rightarrow 2R(-H)(COO^-)O\cdot + O_2 \quad (R7)$$

$$R(-H)(COO^-)O\cdot + O_2 \rightarrow R(-2H)(COO^-)=O + HO_2\cdot \quad (R8)$$

$$R(-H)(COO^-)OO\cdot + HO_2\cdot(H^+ + \cdot O_2^-,\ pK_a = 4.8) \rightarrow R(-H)(COO^-)OOH + O_2 \quad (R9)$$

Reaction R3, the initiation step, is an H atom abstraction from the alkyl chain by ·OH. The issue of whether (R3) involves the direct participation of ·OH(g) (i.e., an Eley−Rideal mechanism) or an ·OH species already accommodated at the interface (i.e., a Langmuir−Hinshelwood mechanism) is discussed below. Note that O_2 is always in excess ($[O_2(g)] = 1.9 \times 10^{18}$ molecules cm^{-3}) over other reactants. The self-reactions of peroxyl radical (R5)−(R7) in bulk aqueous media are known to be extremely fast, with typical rate constants >10^9 M^{-1} s^{-1}.[50] Experiments in D_2O show that the (M + 1) = 175 peak for $R_7(-H)(COO^-)OO\cdot$ is not only the ^{13}C satellite of M but includes a significant contribution from the hydroperoxides $R_7(-H)(COO^-)OOH$ because it partially shifts to m/z = 176 upon deuteration (Figure 3).

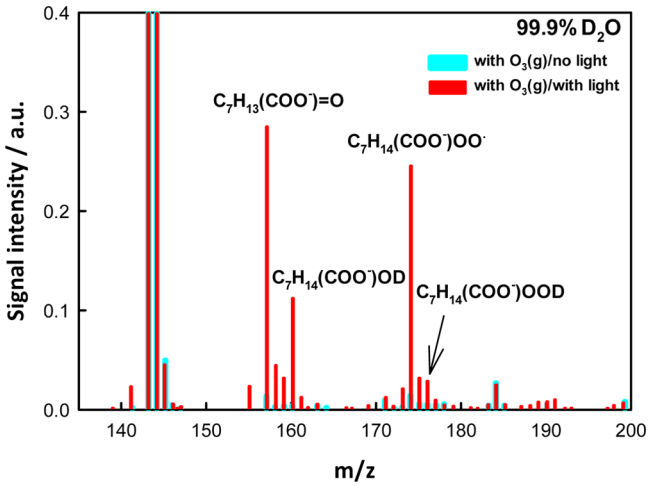

Figure 3. Negative ion electrospray mass spectra of 0.1 mM octanoic acid in 99.9% D_2O microjets exposed to 600 ppmv $O_3(g)$ in $O_2(g)/H_2O(g)/N_2(g)$ mixtures at 1 atm and 298 K. Cyan: laser off. Red: under 40 mJ, ~8 ns pulses (at 10 Hz) of 266 nm radiation ($[\cdot OH]_0 \sim 57$ ppmv). 1 ppmv = 2.46×10^{13} molecules cm^{-3}.

The alcohols $R_7(-H)(COO^-)OH$, which possess exchangeable hydroxyl H atoms with the solvent, are also converted into $R_7(-H)(COO^-)OD$ in D_2O.

The ensuing reactions R4−R9 are deemed to take place in interfacial layers. Because the peroxyls $R(-H)(COO^-)OO\cdot$ cannot abstract H atoms from the reactant $R(COO^-)$ for thermochemical reasons because D(ROO−H) ~ 90 kcal mol^{-1} vs D(R−H) ~ 98 kcal mol^{-1},[51] we consider that the hydroperoxides $R(-H)(COO^-)OOH$ are produced via reaction R9, which involves $HO_2\cdot$, $D(\cdot OO-H) \sim 50$ kcal mol^{-1}. This argument is also consistent with kinetic considerations, because radical−radical reactions $RO_2\cdot + HO_2\cdot$ are relatively fast ($k > 10^7$ M^{-1} s^{-1}),[50] whereas H-abstractions by $RO_2\cdot$ from C−H bonds are much slower (viz., $k = 0.6$ M^{-1} s^{-1} for the linoleate peroxyl radical + cumene reaction in organic solvent).[52] $O(^3P)$ may also abstract H atoms,[53] but with rate constants >50 times smaller than those for ·OH.[42] The fate of $O(^3P)$ is to react with $O_2(g)$ to regenerate O_3 within 50 μs under present conditions.[42] Additional experiments in (1:1) $H_2{}^{16}O$:$H_2{}^{18}O$ mixtures reveal that the O atoms present in the products exclusively arise from gas-phase O-species, because

dx.doi.org/10.1021/jp503387e | J. Phys. Chem. A 2014, 118, 4130−4137

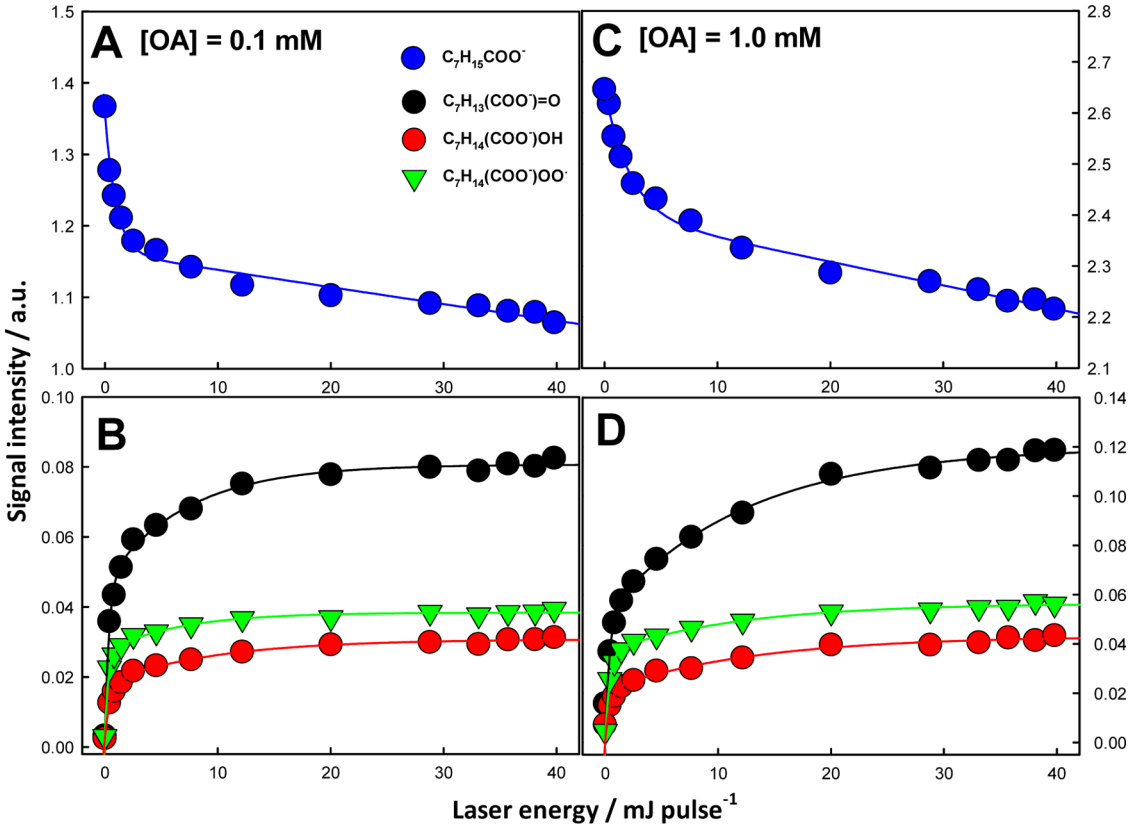

Figure 4. Electrospray mass spectral signal intensities from aqueous 0.1 mM (A, B) or 1.0 mM (C, D) octanoic acid microjets exposed to $O_3(g)/O_2(g)/H_2O(g)/N_2(g)$ mixtures, $[O_3(g)] \sim 600$ ppmv, irradiated with 266 nm laser beams as functions of laser energy (in mJ pulse^{-1}). 1 ppmv = 2.46×10^{13} molecules cm^{-3}.

they do not exchange O with the solvent, as expected from the proposed mechanism and their chemical nature (Figure S2, Supporting Information). We confirmed that reactant depletion and product formation require both the participation of $O_3(g)$ and actinic 266 nm photons (Figure S3, Supporting Information). Because the microjets break up within 10−50 μs after being ejected from the nozzle whereas the laser pulses every 100 ms, we assume the phenomena we observe take place in pristine solutions. Figures 4 and 5 show electrospray mass spectral signals acquired from aqueous 0.1 mM or 1.0 mM OA microjets exposed to irradiated gaseous $O_3/O_2/H_2O/N_2$ mixtures as functions of laser energy per pulse and $[O_3(g)]$, respectively.

In Figure 4, 1, 5, 10, 20, 30, and 40 mJ pulse^{-1} laser pulse energies correspond to $[\cdot OH]_0 \approx 2$, 9, 18, 33, 46, and 57 ppmv colliding with the air−water interface, respectively. It is apparent that reactant losses and concomitant product formation display biexponential behaviors. Significant initial effects are followed by attenuated responses. We interpret these findings as evidence that ·OH rapidly reacts with, and therefore depletes, alkyl chains in the outermost interfacial layers. Thus, above a certain threshold dose, most ·OH would recombine into H_2O_2 in the outermost layers via reaction R10, whereas a only a small fraction reaches the underlying layers to account for the observed attenuated alkyl depletion.

$$2\cdot OH \rightarrow H_2O_2 \qquad \text{(R10)}$$

Because similar behaviors are observed for acetic acid and hexanoic acid (Figure S4 and S5, Supporting Information), we infer that the proposed reaction mechanism applies to all R groups. The ratio of carbonyls to alcohols, R(−2H)(COO^-)=O/R(−H)(COO^-)OH, is larger than 1 under all conditions (Figures 4 and 5). This is taken as evidence of the simultaneous occurrence of the competitive reactions R5, the Russell disproportionation,[54] vs reaction R6, the Bennett−Summers elimination of H_2O_2.[55] The observation that the alcohol R(−H)(COO^-)OH plateaus while the carbonyl R(−2H)-(COO^-)=O keeps increasing as a function of laser energy is consistent with the proposed mechanism, in which the alcohol is produced only from R(−H)(COO^-)OO· + R(−H)(COO^-)-OO· (R5) whereas the carbonyl is formed not only via (R5) but also from R(−H)(COO^-)O· via (R7) and (R8).

Total mass balances (TMB) evaluated before and after laser pulses provide further information on the reactions course. We define TMB as the sum of the products mass signal intensities, which include those of the carbonyls, alcohols, peroxyl radicals, and hydroperoxides, divided by octanoate losses, $[OA]_{without266nm} - [OA]_{with266nm}$. We found that TMB ∼ 0.5 is nearly constant between 0.01 and 1.0 mM [OA] (Figure S6, Supporting Information). This result implies that ∼50% of the products are undetectable via negative ion electrospray mass spectrometry, thereby implying that they escape to gas phase and/or turn neutral. Thus, our results do not exclude the partial fragmentation of reaction intermediates into volatile products either prior to or during detection.[19] We note that neutral products could be formed by electron transfer from the carboxylates to ·OH.[56]

$$RCOO^- + \cdot OH \rightarrow RCOO\cdot + OH^- \qquad \text{(R11)}$$

dx.doi.org/10.1021/jp503387e | J. Phys. Chem. A 2014, 118, 4130−4137

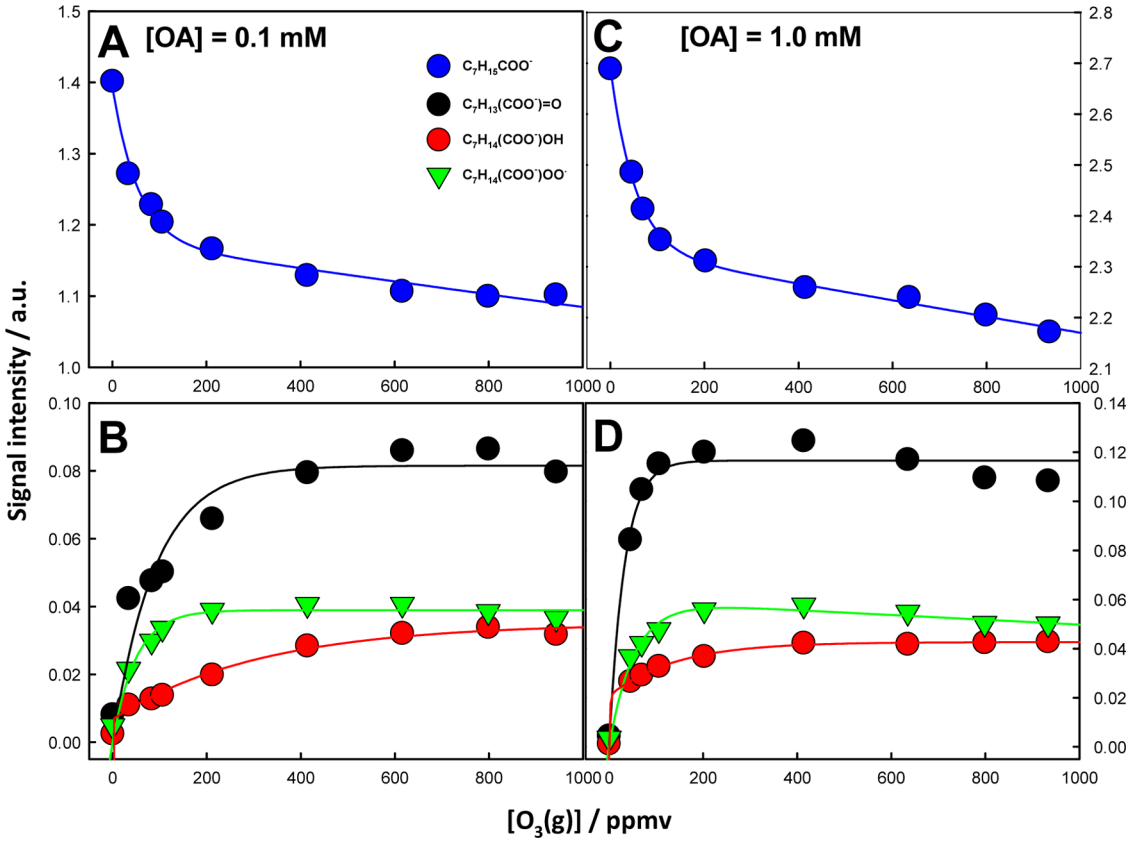

Figure 5. Electrospray mass spectral signal intensities from aqueous 0.1 mM (A, B) or 1.0 mM (C, D) octanoic acid microjets exposed to $O_3(g)/O_2(g)/H_2O(g)/N_2(g)$ mixtures under irradiation by 266 nm laser beams (40 mJ pulse^{-1}) as a function of the $O_3(g)$ mixing ratio; 1 ppmv = 2.46 × 10^{13} molecules cm^{-3}.

Several experimental and theoretical studies have addressed how ·OH(g) is incorporated into interfacial gas−liquid layers. Reported bulk mass accommodation coefficient α values for ·OH(g) on water vary between 0.0035[57] and 0.95,[58] and a surface mass accommodation S = 0.83.[58] Molina et al. reported uptake coefficients $\gamma \sim 0.3$ on reactive humid surfaces of atmospheric importance.[59] If we assume a high $S \sim 0.5$ value on water, it can be shown that on <100 μM OA solutions, ·OH(g) will initially stick to the surface of water and then react with the sparse alkyl chains. The preference of ·OH for the interfacial layers over the bulk[58] should enhance the probability of such events. From the reported adsorption isotherms of OA at the air−water interface,[60] at 50 μM a surface excess $\Gamma \sim 2 \times 10^{-11}$ mol cm^{-2} = 1.2 × 10^{13} molecules cm^{-2} and a surface demand per molecule $A_c \sim 3 \times 10^{-15}$ cm^2 molecule^{-1}, lead to a fractional surface coverage of $\theta \sim 3\%$. Even at 500 μM, where $\theta \sim 70\%$, the surface is not saturated with alkyl chains. By assuming that the radius of a water molecule is 1.4 × 10^{-8} cm, a coverage of $\theta \sim 3\%$ implies that OA molecules at the interface are separated on average by ∼4 × 10^{-7} cm. This is the minimal separation at which the $R_7(-H)(COO^-)OO\cdot$ radical pairs could be formed on the surface via reactions R3 and R4. By assuming a surface diffusion coefficient D = 2 × 10^{-6} cm^2 s^{-1},[61,62] proximal peroxyl radicals would encounter and react via reactions R5−R7 in 0.04 μs, which is about 10^3 times shorter than the lifetime of the microjets on which they reside. Furthermore, because the maximum extent of OA depletion is ∼20% at both 0.1 mM and 1.0 mM, we infer that there is always an excess of ·OH available in the outermost interfacial layers. In a plausible scenario a constant fraction of OA partitions to such layers, regardless of its total concentration, and all such fraction ultimately reacts with excess ·OH. Thus, our results are consistent with a Langmuir−Hinshelwood mechanism rather than an Eley−Rideal mechanism, in agreement with previous studies.[1,19,63]

CONCLUSION

Summing up, we have shown how our novel experimental setup, which combines laser flash photolytic generation of gaseous reactants and surface-sensitive electrospray ionization mass spectrometric detection, lends itself to the study of fast reactions of very reactive, short-lived gas-phase radical species with a wide variety of substrates at the air−water interface. These experiments are conducted under ambient temperature and pressure, in solutions covering a wide concentration range down to the micromolar and provide the unmatched advantage of simultaneous, unambiguous, and mass-based in situ identification of products and intermediates. In this manner, we were able to detect, for the first time, peroxyl and peroxide species in the initial oxidation of organic substrates on aqueous surfaces.

ASSOCIATED CONTENT

Supporting Information

Additional data and experimental details. This material is available free of charge via the Internet at http://pubs.acs.org.

dx.doi.org/10.1021/jp503387e | J. Phys. Chem. A 2014, 118, 4130−4137

AUTHOR INFORMATION

Corresponding Author

*S. Enami: e-mail, enami.shinichi.3r@kyoto-u.ac.jp; phone, +81-774-38-4601.

Notes

The authors declare no competing financial interest.

ACKNOWLEDGMENTS

S.E. is grateful to Kurita Water and Environment Foundation and the Japan Science and Technology Agency (JST) PRESTO program. S.E. also thanks Prof. Hiroshi Masuhara and Dr. Yosuke Sakamoto for stimulating discussions. M.R.H. and A.J.C. acknowledge support from the National Science Foundation (U.S.A.) Grant AC-1238977.

REFERENCES

(1) George, I. J.; Abbatt, J. P. D. Heterogeneous Oxidation of Atmospheric Aerosol Particles by Gas-Phase Radicals. *Nat. Chem.* **2010**, *2*, 713−722.

(2) Donahue, N. M.; Henry, K. M.; Mentel, T. F.; Kiendler-Scharr, A.; Spindler, C.; Bohn, B.; Brauers, T.; Dorn, H. P.; Fuchs, H.; Tillmann, R.; et al. Aging of Biogenic Secondary Organic Aerosol Via Gas-Phase OH Radical Reactions. *Proc. Natl. Acad. Sci. U. S. A.* **2012**, *109*, 13503−13508.

(3) Seinfeld, J. H.; Pandis, S. N. *Atmospheric Chemistry and Physics: From Air Pollution to Climate Change*, 2nd ed.; Wiley: Hoboken, NJ, 2006.

(4) Atkinson, R. Kinetics of the Gas-Phase Reactions of OH Radicals with Alkanes and Cycloalkanes. *Atmos. Chem. Phys.* **2003**, *3*, 2233−2307.

(5) Ziemann, P. J.; Atkinson, R. Kinetics, Products, and Mechanisms of Secondary Organic Aerosol Formation. *Chem. Soc. Rev.* **2012**, *41*, 6582−6605.

(6) Ravishankara, A. R. Heterogeneous and Multiphase Chemistry in the Troposphere. *Science* **1997**, *276*, 1058−1065.

(7) Shiraiwa, M.; Ammann, M.; Koop, T.; Poschl, U. Gas Uptake and Chemical Aging of Semisolid Organic Aerosol Particles. *Proc.Natl. Acad. Sci. U. S. A.* **2011**, *108*, 11003−11008.

(8) Finlayson-Pitts, B. J. Reactions at Surfaces in the Atmosphere: Integration of Experiments and Theory as Necessary (but Not Necessarily Sufficient) for Predicting the Physical Chemistry of Aerosols. *Phys. Chem. Chem. Phys.* **2009**, *11*, 7760−7779.

(9) Donaldson, D. J.; Valsaraj, K. T. Adsorption and Reaction of Trace Gas-Phase Organic Compounds on Atmospheric Water Film Surfaces: A Critical Review. *Environ. Sci. Technol.* **2010**, *44*, 865−873.

(10) Nah, T.; Kessler, S. H.; Daumit, K. E.; Kroll, J. H.; Leone, S. R.; Wilson, K. R. OH-Initiated Oxidation of Sub-Micron Unsaturated Fatty Acid Particles. *Phys. Chem. Chem. Phys.* **2013**, *15*, 18649−18663.

(11) George, I. J.; Abbatt, J. P. D. Chemical Evolution of Secondary Organic Aerosol from OH-Initiated Heterogeneous Oxidation. *Atmos. Chem. Phys.* **2010**, *10*, 5551−5563.

(12) Asmi, E.; Frey, A.; Virkkula, A.; Ehn, M.; Manninen, H. E.; Timonen, H.; Tolonen-Kivimaki, O.; Aurela, M.; Hillamo, R.; Kulmala, M. Hygroscopicity and Chemical Composition of Antarctic Sub-Micrometre Aerosol Particles and Observations of New Particle Formation. *Atmos. Chem. Phys.* **2010**, *10*, 4253−4271.

(13) Tritscher, T.; Dommen, J.; DeCarlo, P. F.; Gysel, M.; Barmet, P. B.; Praplan, A. P.; Weingartner, E.; Prevot, A. S. H.; Riipinen, I.; Donahue, N. M.; et al. Volatility and Hygroscopicity of Aging Secondary Organic Aerosol in a Smog Chamber. *Atmos. Chem. Phys.* **2011**, *11*, 11477−11496.

(14) George, I. J.; Slowik, J.; Abbatt, J. P. D. Chemical Aging of Ambient Organic Aerosol from Heterogeneous Reaction with Hydroxyl Radicals. *Geophys. Res. Lett.* **2008**, *35*, L13811.

(15) Abbatt, J. P. D.; Lee, A. K. Y.; Thornton, J. A. Quantifying Trace Gas Uptake to Tropospheric Aerosol: Recent Advances and Remaining Challenges. *Chem. Soc. Rev.* **2012**, *41*, 6555−6581.

(16) George, I. J.; Vlasenko, A.; Slowik, J. G.; Broekhuizen, K.; Abbatt, J. P. D. Heterogeneous Oxidation of Saturated Organic Aerosols by Hydroxyl Radicals: Uptake Kinetics, Condensed-Phase Products, and Particle Size Change. *Atmos. Chem. Phys.* **2007**, *7*, 4187−4201.

(17) Shiraiwa, M.; Sosedova, Y.; Rouviere, A.; Yang, H.; Zhang, Y. Y.; Abbatt, J. P. D.; Ammann, M.; Poschl, U. The Role of Long-Lived Reactive Oxygen Intermediates in the Reaction of Ozone with Aerosol Particles. *Nat. Chem.* **2011**, *3*, 291−295.

(18) Slowik, J. G.; Wong, J. P. S.; Abbatt, J. P. D. Real-Time, Controlled OH-Initiated Oxidation of Biogenic Secondary Organic Aerosol. *Atmos. Chem. Phys.* **2012**, *12*, 9775−9790.

(19) Vlasenko, A.; George, I. J.; Abbatt, J. P. D. Formation of Volatile Organic Compounds in the Heterogeneous Oxidation of Condensed-Phase Organic Films by Gas-Phase OH. *J. Phys. Chem. A* **2008**, *112*, 1552−1560.

(20) Kolb, C. E.; Cox, R. A.; Abbatt, J. P. D.; Ammann, M.; Davis, E. J.; Donaldson, D. J.; Garrett, B. C.; George, C.; Griffiths, P. T.; Hanson, D. R.; et al. An Overview of Current Issues in the Uptake of Atmospheric Trace Gases by Aerosols and Clouds. *Atmos. Chem. Phys.* **2010**, *10*, 10561−10605.

(21) Cooper, P. L.; Abbatt, J. P. D. Heterogeneous Interactions of OH and HO_2 Radicals with Surfaces Characteristic of Atmospheric Particulate Matter. *J. Phys. Chem.* **1996**, *100*, 2249−2254.

(22) McNeill, V. F.; Yatavelli, R. L. N.; Thornton, J. A.; Stipe, C. B.; Landgrebe, O. Heterogeneous OH Oxidation of Palmitic Acid in Single Component and Internally Mixed Aerosol Particles: Vaporization and the Role of Particle Phase. *Atmos. Chem. Phys.* **2008**, *8*, 5465−5476.

(23) Herrmann, H.; Hoffmann, D.; Schaefer, T.; Brauer, P.; Tilgner, A. Tropospheric Aqueous-Phase Free-Radical Chemistry: Radical Sources, Spectra, Reaction Kinetics and Prediction Tools. *ChemPhysChem* **2010**, *11*, 3796−3822.

(24) Che, D. L.; Smith, J. D.; Leone, S. R.; Ahmed, M.; Wilson, K. R. Quantifying the Reactive Uptake of OH by Organic Aerosols in a Continuous Flow Stirred Tank Reactor. *Phys. Chem. Chem. Phys.* **2009**, *11*, 7885−7895.

(25) Gershenzon, Y. M.; Grigorieva, V. M.; Ivanov, A. V.; Remorov, R. G. O_3 and OH Sensitivity to Heterogeneous Sinks of HOx and CH_3O_2 on Aerosol Particles. *Faraday Discuss.* **1995**, *100*, 83−100.

(26) Enami, S.; Colussi, A. J. Long-Range Specific Ion-Ion Interactions in Hydrogen-Bonded Liquid Films. *J. Chem. Phys.* **2013**, *138*, 184706.

(27) Enami, S.; Colussi, A. J. Long-Range Hofmeister Effects of Anionic and Cationic Amphiphiles. *J. Phys. Chem. B* **2013**, *117*, 6276−6281.

(28) Enami, S.; Hoffmann, M. R.; Colussi, A. J. Dry Deposition of Biogenic Terpenes Via Cationic Oligomerization on Environmental Aqueous Surfaces. *J. Phys. Chem. Lett.* **2012**, *3*, 3102−3108.

(29) Enami, S.; Colussi, A. J. Ion-Specific Long-Range Correlations on Interfacial Water Driven by Hydrogen Bond Fluctuations. *J. Phys. Chem. B* **2014**, *118*, 1861−1866.

(30) Enami, S.; Stewart, L. A.; Hoffmann, M. R.; Colussi, A. J. Superacid Chemistry on Mildly Acidic Water. *J. Phys. Chem. Lett.* **2010**, *1*, 3488−3493.

(31) Enami, S.; Hoffmann, M. R.; Colussi, A. J. Proton Availability at the Air/Water Interface. *J. Phys. Chem. Lett.* **2010**, *1*, 1599−1604.

(32) Mishra, H.; Enami, S.; Nielsen, R. J.; Hoffmann, M. R.; Goddard, W. A.; Colussi, A. J. Anions Dramatically Enhance Proton Transfer through Water Interfaces. *Proc. Natl. Acad. Sci. U. S. A* **2012**, *109*, 10228−10232.

(33) Enami, S.; Sakamoto, Y.; Colussi, A. J. Fenton Chemistry at Aqueous Interfaces. *Proc. Natl. Acad. Sci. U. S. A.* **2014**, *111*, 623−628.

(34) Enami, S.; Mishra, H.; Hoffmann, M. R.; Colussi, A. J. Hofmeister Effects in Micromolar Electrolyte Solutions. *J. Chem. Phys.* **2012**, *136*, 154707.

(35) Cheng, J.; Vecitis, C.; Hoffmann, M. R.; Colussi, A. J. Experimental Anions Affinities for the Air/Water Interface. *J. Phys. Chem. B* **2006**, *110*, 25598−25602.

(36) Ghosal, S.; Brown, M. A.; Bluhm, H.; Krisch, M. J.; Salmeron, M.; Jungwirth, P.; Hemminger, J. C. Ion Partitioning at the Liquid/Vapor Interface of a Multicomponent Alkali Halide Solution: A Model for Aqueous Sea Salt Aerosols. *J. Phys. Chem. A* **2008**, *112*, 12378−12384.
(37) Ghosal, S.; Hemminger, J. C.; Bluhm, H.; Mun, B. S.; Hebenstreit, E. L. D.; Ketteler, G.; Ogletree, D. F.; Requejo, F. G.; Salmeron, M. Electron Spectroscopy of Aqueous Solution Interfaces Reveals Surface Enhancement of Halides. *Science* **2005**, 563−566.
(38) Enami, S.; Hoffmann, M. R.; Colussi, A. J. Prompt Formation of Organic Acids in Pulse Ozonation of Terpenes on Aqueous Surfaces. *J. Phys. Chem. Lett.* **2010**, *1*, 2374−2379.
(39) Sander, S. P.; Friedl, R. R.; DeMore, W. B.; Ravishankara, A. R.; Golden, D. M.; Kolb, C. E.; Kurylo, M. J.; Hampson, R. F.; Huie, R. E.; Molina, M. J.; , et al. *Chemical Kinetics and Photochemical Data for Use in Stratospheric Modeling, Supplement to Evaluation 12: Update of Key Reactions, Evaluation Number 13*; JPL: Pasadena, CA, 2000.
(40) Grebenshchikov, S. Y.; Qu, Z. W.; Zhu, H.; Schinke, R. New Theoretical Investigations of the Photodissociation of Ozone in the Hartley, Huggins, Chappuis, and Wulf Bands. *Phys. Chem. Chem. Phys.* **2007**, *9*, 2044−2064.
(41) Lin, J. J.; Chen, A. F.; Lee, Y. T. UV Photolysis of ClOOCl and the Ozone Hole. *Chemistry—Asian J.* **2011**, *6*, 1664−1678.
(42) *National Institute of Standards and Technology Standard Reference Database Number 69*; NIST: Gaithersburg, MD, 2009.
(43) Dillon, T. J.; Horowitz, A.; Crowley, J. N. The Atmospheric Chemistry of Sulphuryl Fluoride, SO_2F_2. *Atmos. Chem. Phys.* **2008**, *8*, 1547−1557.
(44) Psillakis, E.; Cheng, J.; Hoffmann, M. R.; Colussi, A. J. Enrichment Factors of Perfluoroalkyl Oxoanions at the Air/Water Interface. *J. Phys. Chem. A* **2009**, *113*, 8826−8829.
(45) Cheng, J.; Hoffmann, M. R.; Colussi, A. J. Anion Fractionation and Reactivity at Air/Water: Methanol Interfaces. Implications for the Origin of Hofmeister Effects. *J. Phys. Chem. B* **2008**, *112*, 7157−7161.
(46) Mishra, H.; Enami, S.; Nielsen, R. J.; Stewart, L. A.; Hoffmann, M. R.; Goddard, W. A.; Colussi, A. J. Brønsted Basicity of the Air-Water Interface. *Proc. Nat. Acad. Sci. U. S. A.* **2012**, *109*, 18679−18683.
(47) Enami, S.; Hoffmann, M. R.; Colussi, A. J. Acidity Enhances the Formation of a Persistent Ozonide at Aqueous Ascorbate/Ozone Gas Interfaces. *Proc. Natl. Acad. Sci. U. S. A.* **2008**, *105*, 7365−7369.
(48) *CRC Handbook of Chemistry and Physics*, 90th ed.; CRC Press: Boca Raton, FL, 2010.
(49) Hayase, S.; Yabushita, A.; Kawasaki, M.; Enami, S.; Hoffmann, M. R.; Colussi, A. J. Weak Acids Enhance Halogen Activation on Atmospheric Water's Surfaces. *J. Phys. Chem. A* **2011**, *115*, 4935−4940.
(50) von Sonntag, C.; Schuchmann, H. P. The Elucidation of Peroxyl Radical Reactions in Aqueous-Solution with the Help of Radiation-Chemical Methods. *Angew. Chem., Int. Ed.* **1991**, *30*, 1229−1253.
(51) Colussi, A. J. In *Chemical Kinetics of Small Organic Radicals*; Alfassi, Z. B., Ed.; CRC Press: Boca Raton, FL, 1988; Vol. *1*, pp 25−43.
(52) Porter, N. A.; Lehman, L. S.; Weber, B. A.; Smith, K. J. Unified Mechanism for Poly-Unsaturated Fatty-Acid Autoxidation - Competition of Peroxy Radical Hydrogen-Atom Abstraction, Beta-Scission, and Cyclization. *J. Am. Chem. Soc.* **1981**, *103*, 6447−6455.
(53) Waring, C.; Bagot, P. A. J.; Costen, M. L.; McKendrick, K. G. Reactive Scattering as a Chemically Specific Analytical Probe of Liquid Surfaces. *J. Phys. Chem. Lett.* **2011**, *2*, 12−18.
(54) Russell, G. A. Deuterium-Isotope Effects in the Autoxidation of Aralkyl Hydrocarbons - Mechanism of the Interaction of Peroxy Radicals. *J. Am. Chem. Soc.* **1957**, *79*, 3871−3877.
(55) Hullar, T.; Anastasio, C. Yields of Hydrogen Peroxide from the Reaction of Hydroxyl Radical with Organic Compounds in Solution and Ice. *Atmos. Chem. Phys.* **2011**, *11*, 7209−7222.
(56) Gligorovski, S.; Rousse, D.; George, C. H.; Herrmann, H. Rate Constants for the OH Reactions with Oxygenated Organic Compounds in Aqueous Solution. *Int. J. Chem. Kinet.* **2009**, *41*, 309−326.
(57) Hanson, D. R.; Burkholder, J. B.; Howard, C. J.; Ravishankara, A. R. Measurement of OH and HO_2 Radical Uptake Coefficients on Water and Sulfuric-Acid Surfaces. *J. Phys. Chem.* **1992**, *96*, 4979−4985.
(58) Roeselova, M.; Vieceli, J.; Dang, L. X.; Garrett, B. C.; Tobias, D. J. Hydroxyl Radical at the Air-Water Interface. *J. Am. Chem. Soc.* **2004**, *126*, 16308−16309.
(59) Park, J. H.; Ivanov, A. V.; Molina, M. J. Effect of Relative Humidity on OH Uptake by Surfaces of Atmospheric Importance. *J. Phys. Chem. A* **2008**, *112*, 6968−6977.
(60) Lunkenheimer, K.; Barzyk, W.; Hirte, R.; Rudert, R. Adsorption Properties of Soluble, Surface-Chemically Pure n-Alkanoic Acids at the Air/Water Interface and the Relationship to Insoluble Monolayer and Crystal Structure Properties. *Langmuir* **2003**, *19*, 6140−6150.
(61) Agrawal, M. L.; Neuman, R. D. Surface-Diffusion in Monomolecular Films. 1. Lateral Profile Shift in Radiotracer Method. *J. Colloid Interface Sci.* **1988**, *121*, 355−365.
(62) Agrawal, M. L.; Neuman, R. D. Surface-Diffusion in Monomolecular Films. 2. Experiment and Theory. *J. Colloid Interface Sci.* **1988**, *121*, 366−380.
(63) Bagot, P. A. J.; Waring, C.; Costen, M. L.; McKendrick, K. G. Dynamics of Inelastic Scattering of OH Radicals from Reactive and Inert Liquid Surfaces. *J. Phys. Chem. C* **2008**, *112*, 10868−10877.